BROADBAND MEASUREMENT ANALYSIS OF INDOOR SPACE-TIME CHANNELS

Guido Dolmans[1], **Manel Collados**[2]

[1] *Philips Research Laboratories, WAY 51, Prof. Holstlaan 4, 5656 AA Eindhoven, the Netherlands, email:guido.dolmans@philips.com*

[2] *Philips Research Laboratories, WAY 51, Prof. Holstlaan 4, 5656 AA Eindhoven, the Netherlands, email:manel.collados@philips.com*

ABSTRACT

Multiple-Input-Multiple-Output (MIMO) models often assume no correlation between the elements of the channel matrix. This assumption gives an indication on the upper bound of the channel capacity. However, in practice the channel capacity could decrease when the channels are correlated. In this paper, data measured using a 4x4 MIMO test-bed is processed to extract the spatial correlation in an office environment. In addition, probability density functions of signal strenghts, signal phases, and delay-spreads are measured. The test-bed that has been used is capable of simultaneously capturing 4 receive signals at 5.8 GHz (ISM band of IEEE 802.11a). The bandwidth of the signal is 20 MHz. A detailed description of the test-bed can be found at [1]. In section I, a model for the channel matrix correlation is introduced. This model is used to study the effect of correlation on capacity. In sections II and III the measurement set-up and results are presented.

I. STATISTICAL MODEL AND SIMULATIONS

For a very rich scattering channel, the signals collected at the receive antennas might be considered uncorrelated. However, in practice the receive radio channel signals will be correlated. In this section, Monte Carlo simulation results are presented to predict the sensitivity of capacity to correlated fading.
The MIMO channel matrix with m transmitters and n receivers can be written as

$$\mathbf{H} = \begin{bmatrix} h_{11} & .. & h_{1m} \\ . & & . \\ h_{n1} & .. & h_{nm} \end{bmatrix}, \tag{1}$$

where h_{nm} describes the wireless channel from transmitter m to receiver n.
We adopt the theory of separation of the correlated fading process [2] to the transmit and receive antennas arrays. Using a matrix notation, we construct the following transmit and receiver correlation matrices :

$$\mathbf{R}^{Tx} = \begin{bmatrix} \rho_{11}^{Tx} & .. & \rho_{1m}^{Tx} \\ . & & . \\ \rho_{m1}^{Tx} & .. & \rho_{mm}^{Tx} \end{bmatrix}, \qquad \mathbf{R}^{Rx} = \begin{bmatrix} \rho_{11}^{Rx} & .. & \rho_{1n}^{Rx} \\ . & & . \\ \rho_{n1}^{Rx} & .. & \rho_{nn}^{Rx} \end{bmatrix}, \tag{2}$$

where $\rho_{ij}^{Rx} = |\sum_{k=1}^{m} E\left[h_{ik}h_{jk}\right]/m|$ and $\rho_{ij}^{Tx} = |\sum_{k=1}^{n} E\left[h_{ki}h_{kj}\right]/n|$. The correlation matrix $\mathbf{R}$ of this model is the Kronecker product of the correlation at transmit side and at receive side,

$$\mathbf{R} = \mathbf{R}^{Tx} \otimes \mathbf{R}^{Rx}. \tag{3}$$

The procedure to analyse correlated Rayleigh fading is to generate uncorrelated samples $\mathbf{x}$. From the correlation matrix $\mathbf{R}$, a Choleski decomposition is carried out with $\mathbf{R} = \mathbf{C}\mathbf{C}^{\mathbf{T}}$. The correlated Rayleigh fading samples $\mathbf{z}$ are generated by multiplying $\mathbf{C}$ with the uncorrelated samples $\mathbf{x}$.

For a 2x2 MIMO system, we illustrate this process by taking the following correlation matrices :

$$\mathbf{R}^{Tx} = \begin{bmatrix} 1 & \rho \\ \rho & 1 \end{bmatrix}, \qquad \mathbf{R}^{Rx} = \begin{bmatrix} 1 & \sigma \\ \sigma & 1 \end{bmatrix}, \qquad \mathbf{R} = \begin{bmatrix} 1 & \sigma & \rho & \rho\sigma \\ \sigma & 1 & \rho\sigma & \rho \\ \rho & \rho\sigma & 1 & \sigma \\ \rho\sigma & \rho & \sigma & 1 \end{bmatrix}. \tag{4}$$

The correlation factors ρ and σ take values between 0 (uncorrelated) and 1 (full correlated). The correlated samples $\mathbf{z}$ are grouped together and a correlated fading channel matrix $\mathbf{Z}$ is constructed. The capacity of the MIMO system is obtained from the generalized Shannon equation :

$$C = \log_2 \det \left\{ I + \frac{SNR}{m} \mathbf{Z}\mathbf{Z}^H \right\}. \tag{5}$$

The capacity C versus correlation (with ρ being equal to σ) is calculated using 10k numerically generated samples and is shown in Fig. 1. In this figure, the probability that the capacity is higher than a certain value is displayed. This figure serves as a guideline to get the desired user capacity with a certain reliability.

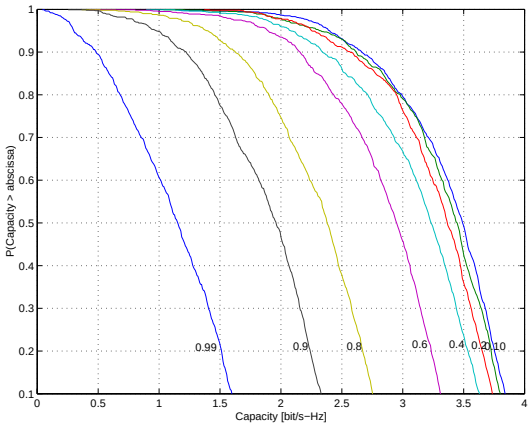

Fig. 1. Correlated Rayleigh fading for $0 < \rho = \sigma < 0.99$ with a signal-to-noise ratio (SNR) of 10 dB

A significant drop in capacity is observed only for $\rho = \sigma > 0.4$.

II. SPATIAL MEASUREMENT SET-UP

The spatial variation in RF signal strength will contain of small-scale and large-scale components. Much attention has been paid in the literature on large-scale fading effects. Our set-up is capable to analyze the small scale effects (distance between spatial points are less than a wavelength) which will show constructive and destructive interference of the radio waves [3], [4]. The spatial MIMO measurement set-up is described in [1].

- The 4 receive antennas are moved through a plane of observation in the indoor propagation environment. The x-y table controller is connected to a Personal Computer (PC). The x-y table position can be controlled very precisely and at each spatial position, the channel matrix $\mathbf{H}$ is measured.
- The 4 transmit antennas are connected via RF and IF chains to multiple D/A cards. The 5.8 GHz signals with 20 MHz bandwidth are transmitted on air.

The amount of collected $\mathbf{H}$ matrices was 1670 in space and 17 taps in time. With the measured database, the amplitude and phase distributions, the delay spread and the correlations ρ and σ are extracted.

III. MEASUREMENT RESULTS

A. Amplitude and Phase Probability Density Functions

Marginal probability-density-functions (PDF) are presented in this section for the magnitude and phase of a (2,2) subset of the channel matrix $\mathbf{H}$. Fig. 2 shows the PDF for the elements magnitude. The empirical PDF is compared with a fitted Rayleigh distribution with parameter b.

The agreement between the Rayleigh distribution and the empirical PDF is quite good. The previous calculation was carried out for the main tap of the channel matrix ; the other taps (pre-echoes and post-echoes) also show spatial fluctuations. The empirical values of the mean value of the power of the discrete impulse response are summarized in Fig. 3, with a tap spacing in time of approximately 62.5 ns. The empirical PDF of the phase of the channel elements are also extracted from the raw measurement data. As an example, the spatial phase PDF is shown in Fig. 4 for matrix element h_{11}. The spatial phase distributions of the other channel matrix elements turned out to be uniform distributed as well.

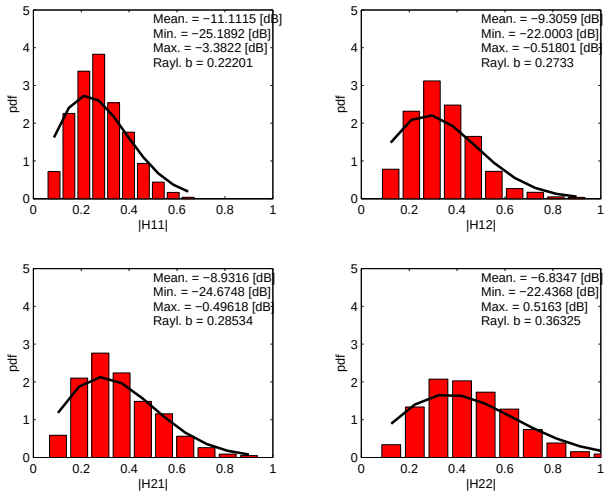

Fig. 2. Empirical 2x2 MIMO spatial amplitude distributions of the main tap.

Echo delay :	Attenuation :
pre-echo -2	-20.3 dB
pre-echo -1	-9.8 dB
main tap	0.0 dB
post-echo +1	-8.5 dB
post-echo +2	-15.0 dB
post-echo +3	-22.1 dB
post-echo +4	-30.2 dB

Fig. 3. Impulse response model of the MIMO channel element h_{11}

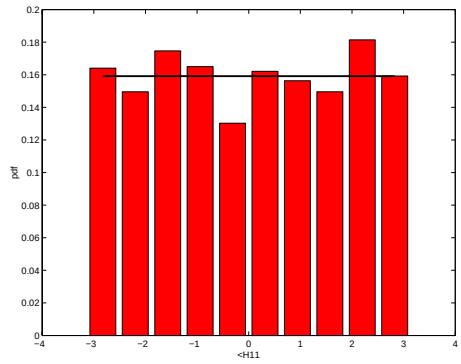

Fig. 4. Empirical 2x2 MIMO spatial phase distribution of the main tap of the main tap of h_{11}

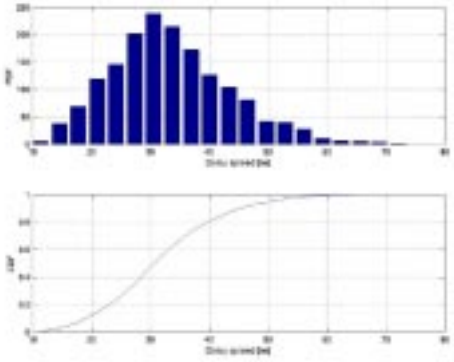

Fig. 5. Delay-spread PDF and CDF

B. **Time-Delay Spread**

From Fig. 3, it is clear that the power in the post and pre-echoes of 5.8 GHz indoor channels cannot be neglected. These echoes will result in distortion (inter-symbol interference) at the receiver, which will influence the bit-error rate of a system. The delay spread will be introduced as a measure of this distortion. The delay spread is taken as the square root of the normalised second central moment of the impulse response. Based on this definition, the empirical probability density function and the cumulative density functions are shown in Fig. 5.
From this figure, it can be concluded that in 99% of the cases, the delay-spread is below 59 ns. In 90% of the cases the delay-spread is below 45 ns and in 50% of the cases, the delay-spread is below 31 ns.

C. **Correlation**

Using the described measurement set-up, 1670 samples of a 4×4 channel have been collected. Each sample consists of 16 channels, one for every transmitter-receiver antenna pair, and every channel consists of 17 taps. From the previous set of samples, subsets of 2×2 elements are selected. Thus, the correlations matrices eventually computed correspond to 2×2 channel matrices. On the other hand, time domain channel responses are translated into frequency domain responses. Frequency samples obtained in this way are treated as different realizations of an equivalent flat sub-channel. According to the measurements, the coherence bandwidth defined for a correlation of 0.5 or higher turns out to be around 10 MHz. Therefore, around two or three independent 10 MHz sub-channel realizations are obtained for each measurement.

$$\boldsymbol{R} = \begin{bmatrix} 1.0000 & 0.1259 & 0.2669 & 0.0661 \\ 0.1259 & 1.0000 & 0.0889 & 0.2503 \\ 0.2669 & 0.0889 & 1.0000 & 0.0933 \\ 0.0661 & 0.2503 & 0.0933 & 1.0000 \end{bmatrix} \quad \hat{\boldsymbol{R}} = \begin{bmatrix} 1.0000 & 0.1096 & 0.2586 & 0.0283 \\ 0.1096 & 1.0000 & 0.0283 & 0.2586 \\ 0.2586 & 0.0283 & 1.0000 & 0.1096 \\ 0.0283 & 0.2586 & 0.1096 & 1.0000 \end{bmatrix}$$

$$\Psi(\boldsymbol{R}, \hat{\boldsymbol{R}}) = 5.1530\ \%$$

Fig. 6. Measured and model correlation matrices when separation between antennas is equal to λ.

In the following we show some correlation results as well as the correlation matrices obtained using the model described in Eq. 3. To determine the quality of the model, we use the same error criteria employed in [5], where the error of the model is defined as

$$\Psi(\boldsymbol{R}, \hat{\boldsymbol{R}}) = \frac{||\boldsymbol{R} - \hat{\boldsymbol{R}}||_F}{||\boldsymbol{R}||_F} \tag{6}$$

being $||\cdot||_F$ the Frobenius norm.
We present the results when both transmitter and receiver antenna pairs are separated one wavelength. The measured correlation matrix is depicted on the left side of Fig. 6. On the right side of the same figure the correlation matrix given by the model is shown. The error of the model using the criterion defined in Eq. 6 is 5.1530 %.
Despite the fact that the error value might seem small, this value must be read carefully. When correlation values are small, as they are in our measurements, the elements in the diagonal of $\boldsymbol{R}$ account for the main part of its F-norm. Thus, the error as defined in Eq. 6 is small as long as the coefficients on the main diagonal of $\hat{\boldsymbol{R}}$ are equal to 1. For example, taking the correlation matrix depicted in Fig.6, and using the identity matrix as $\hat{\boldsymbol{R}}$, the error is around 28 %.
To conclude, in Table I, maximum, minimum, and mean values of model parameters ρ and σ are shown. These values come from the collection of 36 possible valid 2×2 channel sub-matrices that can be extracted from the 4×4 channel measurements.

	Maximum	**Mean**	**Minimum**
ρ	0.2913	0.1649	0.0408
σ	0.2085	0.1060	0.0670

TABLE I
MAXIMUM, MEAN, AND MINIMUM VALUES OF ρ AND σ.

IV. CONCLUSIONS

A test-bed in the 5.8 GHz ISM band with 20 MHz bandwidth is used to measure indoor (4,4) MIMO channels. The test-bed has been used to collect (2,2) MIMO sub-sets channel data. Empirical PDFs of the channel matrix elements and spatial correlation were derived from the indoor channel data. The correlation appears to be below 0.4; therefore the signals are sufficiently decorrelated to exploit the increase of capacity. The Kronecker product model has been applied to measured MIMO data, and the model error turns to be small. It is experienced that correlation values remain constant for antenna spacings larger than one wavelength.

REFERENCES

[1] B. Vandewiele. and P. Mattheijssen, *An Experimental Broadband 4×4 MIMO Test-Bed*, To appear in URSI 2002 General Assembly, Aug 17-24, Maastricht, The Netherlands.
[2] K.I. Pedersen, J.B. Andersen, J.P. Kermoal, and P. Mogensen, *A stochastic Multiple-Input-Output radio channel model for evaluation of space-time coding algorithms*, Proceedings IEEE Vehicular Technology Conference, IEEE VTC Fall, 2000
[3] L. Leyten, *Design of Antenna-Diversity Transceivers for Wireless Consumer Products*, Ph.D. Dissertation, Eindhoven University of Technology, The Netherlands, 2001.
[4] W.M.C. Dolmans, *Effect of Indoor Fading on the Performance of an Adaptive Antenna System*, Ph.D. Dissertation, Eindhoven University of Technology, The Netherlands, 1997.
[5] Kai Yu, Mats Bengtsson, et al. *Measurement Analysis of NLOS Indoor MIMO Channels*, Proceedings IST Mobile Communications Summit pp 277-282, 2001